

Adiabatic Rosen-Zener interferometry with ultracold atoms

Li-Bin Fu,^{1,2} De-Fa Ye,¹ Chaohong Lee,³ Weiping Zhang,⁴ and Jie Liu^{1,2,5}

¹Center for Applied Physics and Technology, Peking University, Beijing 100084, People's Republic of China

²Institute of Applied Physics and Computational Mathematics, Beijing 100088, People's Republic of China

³Nonlinear Physics Center and ARC Center of Excellence for Quantum-Atom Optics, Research School of Physical Sciences and Engineering, Australian National University, Canberra, Australian Capital Territory 0200, Australia

⁴Department of Physics, State Key Laboratory of Precision Spectroscopy, East China Normal University, Shanghai 200062, People's Republic of China

⁵College of Physics and Information Engineering, Hebei Normal University, Shijiazhuang 050016, People's Republic of China

(Received 9 May 2008; published 29 July 2009)

We propose a time-domain “interferometer” based on double-well ultracold atoms through a so-called adiabatic Rosen-Zener process, that is, the barrier between two wells is ramped down slowly, held for a while, and then ramped back. After the adiabatic Rosen-Zener process, we count the particle population in each well. We find that the final occupation probability shows nice interference fringes. The fringe pattern is sensitive to the initial state as well as the intrinsic parameters of the system such as interatomic interaction or energy bias between two wells. The underlying mechanism is revealed and possible applications are discussed.

DOI: [10.1103/PhysRevA.80.013619](https://doi.org/10.1103/PhysRevA.80.013619)

PACS number(s): 37.25.+k, 03.75.Dg, 05.45.-a

I. INTRODUCTION

Quantum interference is one of the most fundamental and challenging principles in quantum mechanics, and has versatile applications in high-precision measurement and quantum coherent control [1–3]. With the development of atom interferometry techniques, researchers are seeking to exploit new interferometric methods using the Bose-Einstein condensate (BEC) [4–6]. In the presence of the nonlinear interaction between the coherent ultracold atoms, the BECs show marvelous nonlinear tunneling and interference properties that are distinguished from the traditional quantum systems. In particular, newly developed techniques in preparing and manipulating BECs in the double well brought a new research surge [7–9].

In this paper, motivated by our recent study on nonlinear Rosen-Zener (RZ) transition [10], we construct an adiabatic Rosen-Zener interferometer using the BECs in the double well by manipulating the height of the barrier between two wells. The Rosen-Zener process was first proposed by Rosen and Zener to account for the spin flip of two-level atoms interacting with a rotating magnetic field in Stern-Gerlach experiments [11]. Here, in our scheme, the RZ process is performed by lowering the barrier between two wells to a height, holding it for a while, and then lifting it back to the original height. We suppose initially that the barrier is very high so that the ground state (GDS) and first-excited state (FES) are degenerate. When the barrier is lowered, the tunneling between two wells will break the degeneracy. Hence, the above scheme is a Mach-Zehnder interferometer; lowering and lifting of the barrier just corresponds to beam splitting and recombining process, respectively (see Fig. 1 for details).

Our paper is organized as follows. In Sec. II, we present our nonlinear Rosen-Zener interferometer scheme. In Sec. III, we demonstrate Rosen-Zener interference effect with BECs in double well and make thoroughly theoretical

analysis on the nonlinear process. In Sec. IV we study the spatial interference effects during Rosen-Zener process.

II. ROSEN-ZENER INTERFEROMETRY WITH BECS IN A DOUBLE-WELL

We consider a Bose atomic condensate trapped in a double-well potential with strongly transverse confinement, the dynamics obeys a one-dimensional model

$$i\hbar \frac{\partial}{\partial t} \Psi(x,t) = H_0 \Psi(x,t) + \lambda |\Psi(x,t)|^2 \Psi(x,t), \quad (1)$$

where $H_0 = -(\hbar^2/2m)(\partial^2/\partial x^2) + V(x)$, $\lambda = 8N\pi\hbar^2\beta_{1d}a_s/m$, m is the single-atom mass, a_s is the s -wave scattering length describing the interatom interaction, N is the total particle number, and β_{1d} is the compensating coefficient for reducing transverse freedoms. $V(x)$ is a double-well potential realized

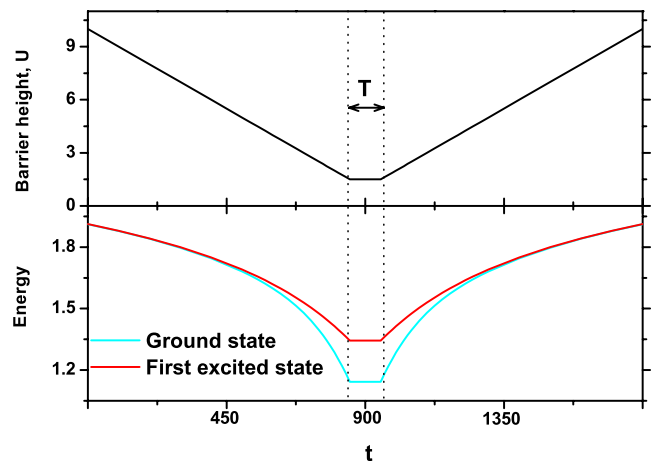


FIG. 1. (Color online) Schematic diagram for an adiabatic RZ process. Upper panel: the barrier height between two wells in time sequence. Bottom panel: the energies of the ground state and the first-excited state in time with varying barrier.

by superposing a Gaussian barrier to a harmonic trap

$$V(x) = \frac{1}{2}\omega^2 x^2 + U \exp\left(-\frac{x^2}{2d^2}\right), \quad (2)$$

in which ω is the trapping frequency of harmonic potential, d is the barrier width, and U is the barrier height. In the Rosen-Zener process we control the barrier height as follows:

$$U = \begin{cases} U_0 - \alpha t & \text{for } 0 < t < t_1, \\ U_h & \text{for } t_1 < t < t_2, \\ U_h + \alpha t & \text{for } t_2 < t < t_f, \end{cases} \quad (3)$$

where α is the ramping rate, $t_1 = (U_0 - U_h)/\alpha$, $t_2 = t_1 + T$, $t_f = 2t_1 + T$, and T is the holding time (see Fig. 1).

During the whole process above, the barrier is changed very slowly so that the excitation to high eigenstates is very small. We assume that the system only occupies the ground and first-excited states during the adiabatic process, i.e., $\Psi(x, t) = c_0(t)\Psi_g(x, U) + c_1(t)\Psi_e(x, U)$ where $\Psi_g(x, U)$ and $\Psi_e(x, U)$ are the GDS and FES for Gross-Pitaevskii (GP) equation (1) with the barrier height U , which obeys $E_j\Psi_j = H_0\Psi_j + \lambda\Psi_j^3$, where E_j is the chemical potential for Ψ_j ($j=e, g$). When the barrier is very high, the two wells are almost independent and no atoms exchange between wells, so we can have two stable local modes, $|\Psi_L\rangle = \frac{1}{\sqrt{2}}(|\Psi_g\rangle - |\Psi_e\rangle)$ and $|\Psi_R\rangle = \frac{1}{\sqrt{2}}(|\Psi_g\rangle + |\Psi_e\rangle)$, for which almost all the atoms are localized in one well. Because the excitations to high eigenstates are very small, the atoms will still occupy only on the ground state and the first-excited state at final, $|\Psi_f\rangle = c_0|\Psi_g\rangle + c_1|\Psi_e\rangle$, i.e., $|\Psi_f\rangle = a|\Psi_L\rangle + b|\Psi_R\rangle$ with $a = \frac{1}{\sqrt{2}}(c_0 - c_1)$ and $b = \frac{1}{\sqrt{2}}(c_0 + c_1)$, in which $|c_0|^2 + |c_1|^2 = 1$. Therefore, the final probabilities on the left and right wells are

$$|a|^2 = \frac{1}{2} - |c_0||c_1|\cos\theta, \quad |b|^2 = \frac{1}{2} + |c_0||c_1|\cos\theta, \quad (4)$$

where $\theta = \arg(c_1) - \arg(c_0)$. The final occupation of one well serves as the interferometer ‘‘output ports,’’ which is the interference between the ground state and the first-excited state.

III. INTERFERENCE BETWEEN DEGENERATED EIGENSTATES AND PHASE LOCKING EFFECT

In this section, we discuss the dynamics of the nonlinear Rosen-Zener process with a simple model. Defining $z = |c_1|^2 - |c_0|^2$ and $\theta = \arg(c_1) - \arg(c_0)$, the total energy of the system, $H = \int [\Psi^\dagger(x)H_0\Psi(x) + \frac{\lambda}{2}|\Psi(x)|^4]dx$, can be expressed in terms of z and θ as

$$H = \delta z + \frac{\beta}{2}z^2 + \Lambda(1 - z^2)\cos^2\theta, \quad (5)$$

in which $\delta = E_e - E_g + \frac{1}{2}(\gamma_{gg} - \gamma_{ee})$, $\beta = \frac{1}{2}(\gamma_{ee} + \gamma_{gg} - 2\gamma_{eg})$, $\Lambda = \gamma_{eg}$, and $\gamma_{ij} = \lambda \int \Psi_i^2 \Psi_j^2 dx$ ($i, j = e, g$). In the above deductions, the integrals with odd powers of Ψ_e and Ψ_g are nearly zero and have been omitted [12]. In the upper panel of Fig. 2, we plot $E_e - E_g$, γ_{ij} as functions of the barrier height U .

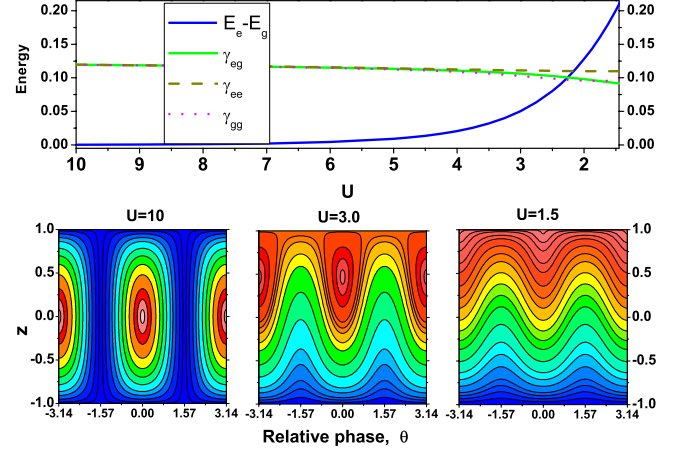


FIG. 2. (Color online) The upper panel is for γ_{gg} , γ_{eg} , γ_{ee} , and $E_e - E_g$ for different barrier heights with the same parameters for Fig. 2. The bottom row shows three phase spaces of classical Hamiltonian (5) for $U=10, 3, 1.5$, respectively.

The total energy serves as a classical Hamiltonian with the canonically conjugate variables z and θ . The equations for z and θ are

$$\dot{z} = -\frac{\partial H}{\partial \theta}, \quad \dot{\theta} = \frac{\partial H}{\partial z} \quad (6)$$

[the two equations can be also directly obtained from GP equation (1)]. This classical Hamiltonian system has two axial fixed points at $z = \pm 1$ independent of the relative phase, in which $z = -1$ corresponds to the ground state of GP equation (1) and $z = +1$ corresponds to the first-excited state. The other fixed points of the above classical Hamiltonian can be obtained by solving the equation $\dot{z} = 0$ and $\dot{\theta} = 0$. For $\delta < (\Lambda - \beta)$, we obtain $(z^*, \theta^*) = (\frac{\delta}{\Lambda - \beta}, 0)$ and $(z^*, \theta^*) = (\frac{\delta}{\Lambda - \beta}, \pi)$. These two fixed points just correspond to the so-called self-trapping states in double-well systems [13–17]. If the barrier is low enough, $\delta > (\Lambda - \beta)$, the two fixed points will merge into the first-excited states, i.e., $z = 1$. In the bottom row of Fig. 2, we show the phase spaces of classical Hamiltonian (5) for three typical values of barrier heights.

Using these equations with the barrier U varying, the parameters depending on U read from Fig. 2; we simulate evolution of the system numerically by fourth to fifth order Runge-Kutta algorithm. In the following we choose dimensionless parameters as: the trapping frequency $\omega = 0.2\pi$, the barrier width $d = 1/\sqrt{2}$, the initial and final heights $U_0 = U_f = 10$, the lowest height $U_h = 1.5$, and the ramping rate $\alpha = 0.01$.

We consider when the BECs are initially localized in one well (e.g., the right one) and the barrier between two wells is sufficiently high. In Fig. 3, we plot two typical probability evolutions in the left column, and the final probabilities and relative phase θ versus holding time T in the right column. The left column shows the density (the upper) and relative phase θ (the bottom) evolution during the RZ process for the holding time $T = 110$ and $T = 120$, respectively. From the cal-

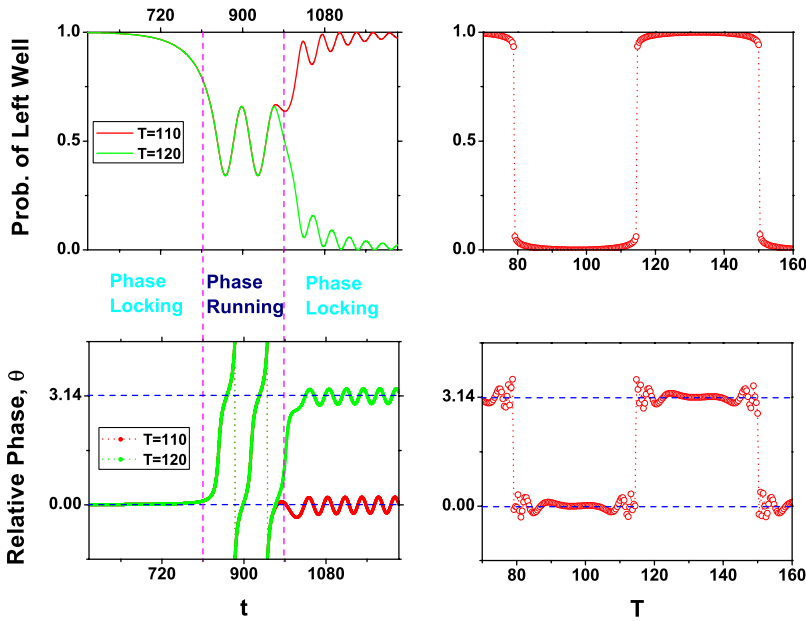


FIG. 3. (Color online) Numerical results for the transfer probability and relative phase obtained by classical system (5). The left column shows the time evolutions for $T=110, 120$. The right column exhibits the dependence of final occupations and phases on T .

culations we see that, as the barrier lowers, the tunneling between two wells occurs, and the macroscopic quantum tunneling (Josephson oscillation) is clearly visible. At this stage, the phase locking is destroyed by the tunneling. It is interesting that the phase locking state will be revived when the barrier is increased back. Finally, all atoms completely localize in one well again; however, it does not always come back to the initial well. Which well will be occupied depends on the holding time, and the final occupation probabilities form a rectangle function of T (see the right panel of Fig. 3).

The above results can be well understood with adiabatic approximation. The system is initially fully localized in the right well, i.e., initially at the fixed point $(z^*, \theta^*) = (0, 0)$. As the barrier height decreases slowly, the system evolves along the fixed point $(z^*, \theta^*) = (\frac{\delta}{\Lambda - \beta}, 0)$ until the barrier height is so low that $\delta > \Lambda - \beta$. At this time, we hold the barrier unchanged for time T . During the holding stage, the state evolves close to the first-excited state with relative phase θ running. Also, one can see the Josephson oscillation during this stage. As the barrier height is raised up again, the running phase orbit will drop into phase locking orbit around one of the two fixed points. On the other hand, since the initial state is a fixed point, the adiabatic evolution guarantee the final state should be close to one of the two fixed points $(0, 0)$ or $(0, \pi)$ [18]. Because of the symmetry, the probability for dropping into these two phase locking regions is the same. The period of the rectangular function is determined by the period of the running phase orbit when the barrier is held. From the classical model, the period can be calculated theoretically, which is $\frac{2\pi}{\sqrt{(\delta - \beta)^2 - \Lambda^2}}$ (in which the parameters are chosen as the values for the holding stage), and for the above case it is about 35, which consists of the above calculation very well. Obviously, the period can be controlled by the interatom interaction (s -wave scattering length) and the barrier height.

By directly solving GP equation (1) using the operator-splitting approach, we reproduce the above results. In Fig. 4, we plot two typical probability evolutions in the upper panel

column, and the final probabilities versus T in the bottom. These figures show that the phenomena predicted above can be well verified by the GP equation.

The nonlinearity plays an important role in the above interesting processes. If there is no nonlinearity, i.e., $\Lambda = \beta = 0$, the system will become very simple with the Hamiltonian as $H = \delta z$. The solution of such linear case can be obtained easily: $z = z(0)$, $\theta = \int_0^t \delta(t) dt$. Then from Eq. (4) we can get the final probabilities of both wells. In Fig. 5, we plot two typical probability evolutions in the left column, and the final probabilities and relative phase θ versus holding time T in the right column, the parameters are the same as in Fig. 3 except for $\Lambda = \beta = 0$. From these figures we see that for the interaction-free case the final probabilities of one well are oscillating between zero and one during the Rosen-Zener process. On the other hand, there is a critical value of the interaction for which one has $\delta_{\max} > \Lambda - \beta$, where δ_{\max} is the maximal value of δ during the Rosen-Zener process. Only this condition is satisfied; the transition between the phase

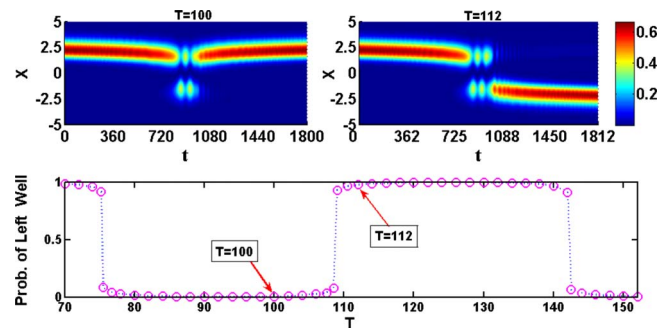


FIG. 4. (Color online) Coherent transition of atoms by the RZ process. The upper figures give two example of such a process. For the holding time $T=100$ (left figure), atoms are still in the initial well; however, for $T=112$ (right one) almost all atoms are transferred to another well. The lower panel shows the probabilities of occupation on the left well for different holding times T (all atoms in right well initially)

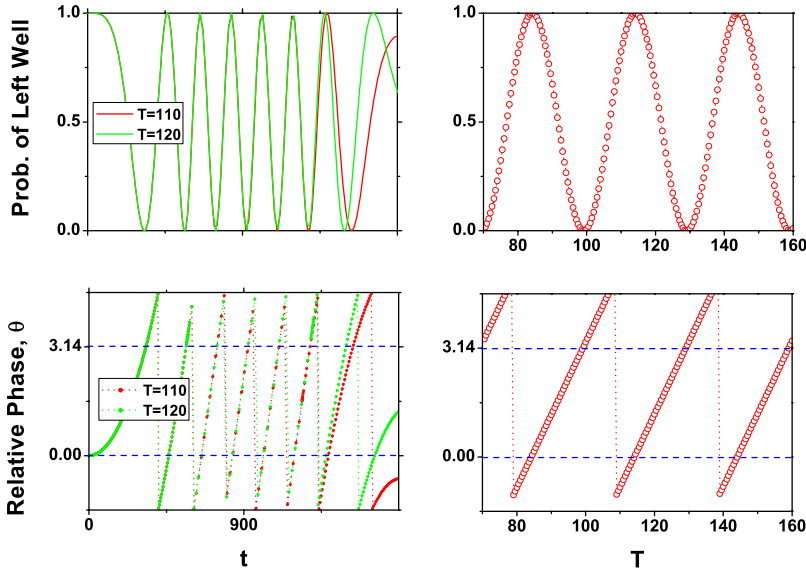


FIG. 5. (Color online) The RZ processes for interaction-free case. The left column shows the time evolutions for $T=110, 120$. The right column exhibits the dependence of final occupations and phases on T .

locking state and running phase state will occur, then the final occupation probabilities will be a rectangle function of T .

IV. INTERFERENCE OF SPATIAL MODES

Another interesting case is for the atoms populating evenly in two wells (e.g., ground state). These states are for the atoms populating evenly in two wells, i.e., $|\Psi_0\rangle = \frac{1}{\sqrt{2}}(|\Psi_L\rangle + e^{i\xi}|\Psi_R\rangle)$. For such a case, the population imbalance after the RZ process is determined by both the holding time T and the initial phase difference ξ , the latter can be controlled with the “phase-imprinting” technique of shining two laser beams with different intensity [19]. Figure 6, calculated by Hamiltonian system (5), exhibits the final populations in the left well versus the holding time T for different ξ (the top row), and the populations versus ξ for $T=100$ and 150 (the second row). These figures show that, after carrying out the RZ scheme, the final population occupations of the two wells depend on the relative phase ξ as well as the holding time T . In particular, for a fixed ξ , the final occupations vary with the holding time T , showing a nice interference pattern in the time domain. The interference pattern depends on the nonlinear interaction and reduces to a sinusoidal function in the absence of interatom interaction.

Time-resolved interferometry is a conventional method to measure the relative phase [20]. From the above simulations, we find that the final occupations on the two wells sensitively depend on the initial conditions. Hence, we should extract the initial information from the final occupations. However, from Fig. 6 one sees that for a given holding time T the final occupations are not single valued about initial phases. Therefore, to extract initial phase we need to carry it out at least twice with different holding times. On the other hand, in designing a RZ scheme, one could realize the double-well BECs with definite population imbalance and relative phase serving as coherent matter wave source used for other practical purpose.

The numerical results also show that the final occupations are sensitive to the phase ξ , especially around $\xi=\pi$. Thus

around the first-excited state, the evolution is very sensitive to the initial condition. These results are supported by directly solving the GP equation. The bottom two rows of Fig. 6 are the density evolutions for $\xi=1.01\pi$ and 1.02π , respec-

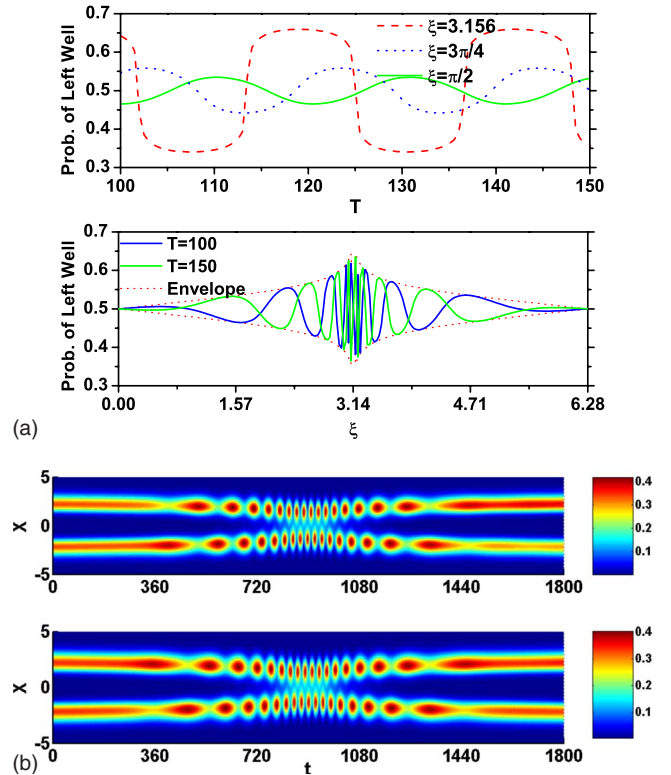


FIG. 6. (Color online) The upper panel plots the final transfer probabilities of different initial relative phase ξ vs the holding time T calculated with the classical model. The second row plots the final transfer probabilities vs different initial relative phase ξ for $T=100$ and 150 . The dotted line is the envelope for the extreme values of every ξ when changing the holding time T . The next two rows are two examples obtained by directly solving the GP equation for $\xi=1.01\pi$ and 1.02π , respectively.

tively, obtained by the GP equation, from which this sensitivity can be found.

V. DISCUSSIONS

In summary, a scheme for an interferometer with the matter wave in a double-well potential serving as coherent sources is proposed. This scheme is realizable with present experimental techniques. With it, the population imbalance of the atoms in two wells shows interesting interference patterns in the time domain. The fringe pattern is sensitive to the initial state, the interatomic interaction, and the external forces such as gravity, which can change the shape of the double well. In this sense, this interferometric scheme has the potentials for precision measurements with ultracold atoms.

ACKNOWLEDGMENTS

This work was supported by National Natural Science Foundation of China (Grants No. 10725521, No. 10604009, No. 10588402, and No. 10474055), the National Fundamental Research Programme of China under Grants No. 2006CB921400, No. 2006CB921104, and No. 2007CB814800, and the Australian Research Council (ARC). W.Z. also acknowledges funding by the Science and Technology Commission of Shanghai Municipality under Grants No. 06JC14026 and No. 05PJ14038, the Program of Shanghai Subject Chief Scientist under Grant No. 08XD14017, the Program for Changjiang Scholars and Innovative Research Team in University, Shanghai Leading Academic Discipline Project under Grant No. B480, and the Research Fund for the Doctoral Program of Higher Education No. 20040003101.

-
- [1] A. Peters, K. Y. Chung, B. Young, J. Hensley, and S. Chu, *Philos. Trans. R. Soc. London, Ser. A* **355**, 2223 (1997).
- [2] B. P. Anderson and M. A. Kasevich, *Science* **282**, 1686 (1998).
- [3] M. S. Chapman, T. D. Hammond, A. Lenef, J. Schmiedmayer, R. A. Rubenstein, E. Smith, and D. E. Pritchard, *Phys. Rev. Lett.* **75**, 3783 (1995); C. R. Ekstrom, J. Schmiedmayer, M. S. Chapman, T. D. Hammond, and D. E. Pritchard, *Phys. Rev. A* **51**, 3883 (1995).
- [4] M. R. Andrews *et al.*, *Science* **275**, 637 (1997).
- [5] Y. Shin, M. Saba, T. A. Pasquini, W. Ketterle, D. E. Pritchard, and A. E. Leanhardt, *Phys. Rev. Lett.* **92**, 050405 (2004); T. Schumm *et al.*, *Nat. Phys.* **1**, 57 (2005).
- [6] F. S. Cataliotti *et al.*, *Science* **293**, 843 (2001).
- [7] G.-B. Jo, Y. Shin, S. Will, T. A. Pasquini, M. Saba, W. Ketterle, D. E. Pritchard, M. Vengalattore, and M. Prentiss, *Phys. Rev. Lett.* **98**, 030407 (2007); G.-B. Jo, J.-H. Choi, C. A. Christensen, T. A. Pasquini, Y.-R. Lee, W. Ketterle, and D. E. Pritchard, *ibid.* **98**, 180401 (2007).
- [8] R. Gati, B. Hemmerling, J. Fölling, M. Albiez, and M. K. Oberthaler, *Phys. Rev. Lett.* **96**, 130404 (2006).
- [9] A. Günther, S. Kraft, C. Zimmermann, and J. Fortágh, *Phys. Rev. Lett.* **98**, 140403 (2007).
- [10] D. F. Ye, L. B. Fu, and J. Liu, *Phys. Rev. A* **77**, 013402 (2008).
- [11] N. Rosen and C. Zener, *Phys. Rev.* **40**, 502 (1932).
- [12] D. Ananikian and T. Bergeman, *Phys. Rev. A* **73**, 013604 (2006).
- [13] M. Albiez, R. Gati, J. Fölling, S. Hunsmann, M. Cristiani, and M. K. Oberthaler, *Phys. Rev. Lett.* **95**, 010402 (2005).
- [14] A. Smerzi, S. Fantoni, S. Giovanazzi, and S. R. Shenoy, *Phys. Rev. Lett.* **79**, 4950 (1997); S. Raghavan, A. Smerzi, S. Fantoni, and S. R. Shenoy, *Phys. Rev. A* **59**, 620 (1999).
- [15] G. J. Milburn, J. Corney, E. M. Wright, and D. F. Walls, *Phys. Rev. A* **55**, 4318 (1997).
- [16] E. A. Ostrovskaya, Y. S. Kivshar, M. Lisak, B. Hall, F. Cattani, and D. Anderson, *Phys. Rev. A* **61**, 031601(R) (2000); C. Lee, W. Hai, X. Luo, L. Shi, and K. Gao, *ibid.* **68**, 053614 (2003); C. Lee, W. Hai, L. Shi, and K. Gao, *Phys. Rev. A* **69**, 033611 (2004).
- [17] L.-B. Fu and J. Liu, *Phys. Rev. A* **74**, 063614 (2006); G.-F. Wang, L.-B. Fu, and J. Liu, *ibid.* **73**, 013619 (2006).
- [18] J. Liu, B. Wu, and Q. Niu, *Phys. Rev. Lett.* **90**, 170404 (2003); L.-B. Fu and S.-G. Chen, *Phys. Rev. E* **71**, 016607 (2005); J. Liu, L. Fu, B. Y. Ou, S. G. Chen, D. I. Choi, B. Wu, and Q. Niu, *Phys. Rev. A* **66**, 023404 (2002).
- [19] J. Denschlag *et al.*, *Science* **287**, 97 (2000).
- [20] B. R. da Cunha and M. C. de Oliveira, *Phys. Rev. A* **75**, 063615 (2007).